

Synthesis and Characterization of Chitosan-Herbal (*Aloe vera*) Bionanocomposite towards the Development of Medical Apparels

R. Chakraborty^{*1}, Dr. S. Chatterjee², Dr. A. Chakraborty³

¹Department of Medical Lab Technology, Supreme Knowledge Foundation Group of Institutions, Mankundu - 712139, Hooghly, West Bengal, India

²Department of Biotechnology, Techno India University, EM-4, Sector-V, Salt Lake, Kolkata – 700 091, West Bengal, India.

³Department of Textile Technology, Govt. College of Engineering and Textile Technology, Serampore – 712 201, West Bengal, India

Abstract

The synthesis and characterization of bionanocomposite have garnered significant attention due to their versatile application in the field of scientific and medical apparels. In the present study, a novel bionanocomposite was synthesized using chitosan and *Aloe vera* in presence of sodium tripolyphosphate (STPP) as cross linking agent. The structural characterization of synthesized chitosan-herbal (*Aloe vera*) bionanocomposite (CHBNC) was carried out by analysing UV-Visible, Fourier Transform Infrared (FTIR), Nuclear Magnetic Resonance (NMR) (¹H, ¹³C and ³¹P) spectra which finally confirmed the composite nature of CHBNC. The thermal and surface morphology characterization of obtained composite were conducted on Differential Scanning Calorimetry (DSC), Thermo Gravimetric Analyzer (TGA), Scanning Electron Microscope (SEM) and Atomic Force Microscope (AFM). The results showed higher thermal stability of CHBNC as compared to chitosan and *Aloe vera* alone. Analysis of SEM, AFM and Dynamic Light Scattering (DLS) results indicated rough surface morphology and spherical shape of CHBNC particles with average particle diameter of about 48.73 nm.

Keywords: Chitosan, *Aloe vera*, Bionanocomposite, UV-visible, FTIR, NMR, SEM, AFM, DLS.

* Corresponding author

R. Chakraborty

Department of Medical Lab Technology, Supreme Knowledge Foundation Group of Institutions, Mankundu - 712139, Hooghly, West Bengal, India.

Introduction

With the development of science and technology and the improvement in living standard, people have continuously strengthened their awareness on health and environmental protection of clothing [1]. Cotton fabric has been used as a textile material for centuries and favour of people due to its healthy, environment protecting character, feel, airy, soft elegant appearance, and eximious performance of absorbing moisture, good hand feel and comfortability for wear. However, cotton fabrics, especially those in contact with human body offer an ideal environment for microbial growth because of their large surface area and ability to retain moisture. Moreover, carbohydrates in cotton can act as nutrient and energy sources under certain conditions. Soil, dust, solutes from sweat and some textile finishes can also be nutrient sources for micro-organisms [2]. The growth of microorganisms on textiles inflicts a range of unwanted effects not only on the textiles itself but also on the wearer. These effects include the generation of obnoxious smell from inner garment, spread of diseases, stains and discolouration in the fabric, a reduction in mechanical strength and an increased likelihood of contamination. For these reasons, it is highly desirable that the growth of microbes on textiles be minimized during the storage and use. The consumers are now increasingly aware of the hygienic life style and there is a necessity and expectation of wide range of textile products finished with antimicrobial properties. Various antimicrobial agents are currently available in the market with a wide range of antimicrobial properties under different trade names for textile industry. These chemicals include inorganic salts, organometallics, iodophors (substances that slowly release iodine), phenols and thiophenols, onium salts, antibiotics, heterocyclics with anionic groups, nitro compounds, ureas and related compounds, formaldehyde derivatives and amines [3]. Many of these chemicals, however, are toxic to humans and do not easily degrade in the environment.

The textile industry continues to look for eco-friendly processes that substitute for toxic textile chemicals [4-6]. Recently, natural materials like chitosan, natural dyes, herbal products such as *Aloe vera*, tea tree oil, eucalyptus oil, tulsi and neem leaf extracts are attracting the attention of researchers because of their availability of resources, low cost, easy handling and minimum damage to the environment. In addition, they have unique properties such as non-toxicity and biological degradability. Nowadays, chitosan, a natural linear bio-polyamino saccharide has opened up a new avenue in this area of research and has also been studied as a new antibacterial agent for textiles [7]. Among herbal products, *Aloe vera* has emerged out as the best one due to the presence of acemannan, the most bioactive polysaccharide in it.

Chitosan and *Aloe vera* alone in nano form show good antimicrobial property without showing any improvement in water and blood repellence which are important parameters for medical apparels as they cannot form nano whiskers of appropriate length to develop the same. In order to cope up with the problems it has been thought worthwhile to synthesize and characterize chitosan-*Aloe vera* bionanocomposite so that each of the components can work synergistically for achieving the required nano composite along with significantly higher length of nano whiskers in view of the development of medical apparels

Materials and Methods

Materials

Leaves of *Aloe vera* (*Aloe barbadensis* Miller) (supplied by Bishnuchandra Nursery, Hooghly, West Bengal, India), reagent grade chitosan (supplied by Hi-media, Mumbai, India, molecular weight 166 kDa, viscosity 1860 cP, degree of deacetylation 81%), sodium tri poly phosphate (STPP), hydrochloric acid (35%), ethanol (95%), deionized water, acetic acid (99.8%), tween 80, span 80, palm oil, phosphate buffer tablet and petroleum ether (supplied by Unichem Supply Agency, Kolkata, West Bengal, India) were used .

Methods

Preparation of chitosan solution

Chitosan solution (3%) was prepared by mixing 3 g of chitosan in acetic acid solution (3%) with the help of magnetic stirrer at 60°C for 12 h. In order to remove air bubbles the resultant solution was kept overnight as such.

Gel extraction from *Aloe vera* leaves

Fresh *Aloe vera* leaves obtained from *Aloe vera* plant (*Aloe barbadensis* Miller) were washed thoroughly with distilled water to remove dirt, dust and other foreign particles from the surface. Then the weight of the leaves was taken and it was found to be 2 kg. The leaves were then cut in the middle. The outer green dermis of the leaf was peeled off from the parenchyma using a sterile knife. The inner flesh or gel was then cut into small pieces and washed with distilled water. After that, the gel so obtained was weighed which was found to be 480 g and kept at 4°C for 2 h.

Isolation of main functional component (acemannan) from *Aloe vera* gel

The main functional component acemannan was isolated from *Aloe vera* gel as per method described elsewhere [8].

The clear gel was homogenized with a polytron hand held homogenizer (Model PT1200E, Switzerland). To the obtained gel, dilute hydrochloric acid (10%) was added slowly under mild agitation until the pH of the mixture reached to 4. Calcium oxalates, magnesium oxalates, calcium lactates and magnesium lactates so present within the gel as impurities were eliminated in the process through solubilization. Ethanol (95%) was added slowly to the resultant solution till the volume ratio of ethanol and gel solution reached to 4:1 and worked for 5-6 h at room temperature. During this treatment, anthraquinones, monosugars, inorganic salts, organic acids and oligosaccharides were eliminated as they are soluble in ethanol-water mixture. Finally, the solution was kept under stand still condition for 24 h for better precipitation and maximum yield.

The fibroid mooring materials were removed and then centrifugation (Labtechnik, Telangana, India) was carried out at 10,000xg. The precipitate was then dissolved in deionized water and passed through MF-Millipore Membrane (Merck 0.22 µm pore size) filter using high pressure vacuum pump filtration (Millipore), lyophilized (Lyophilizer, C-Gen Biotech, Pune, India) and stored at -20°C for further use. The yield of acemannan was found to be 2.98 g.

Synthesis of chitosan-herbal (*Aloe vera*) bionanocomposite (CHBNC)

Chitosan-herbal (*Aloe vera*) bionanocomposite was prepared using Multiple Emulsion Solvent Evaporation (MESE) procedure. To the prepared chitosan solution 15 ml of *Aloe vera* extract (20% solution of isolated acemannan) was added drop wise at room temperature under slow stirring and worked for 15 min which finally gave out an off white coloured precipitate of chitosan-herbal composite (CHC). The precipitate was filtered and air dried. Then 3% CHC solution was mixed with 5% Tween 80 solution and put onto a rotary shaker for 5 min. On the other hand, 5% Span 80 solution was prepared by stirring 5 ml of Span 80 with 95 ml of palm oil for a period of 10 min. Then, 9 parts of the first solution were mixed with 1 part of the second solution and stirred well for 5 min. To this, 0.01g of STPP was then added with slow stirring for 5 min. A cream coloured suspension formed which was subjected to incubation for 1 h at 50°C. This was followed by cooling to bring down the temperature of suspension at room temperature. A pale yellow coloured CHBNC layer (in ring form) formed at the top of suspension which was washed with petroleum ether in order to separate it out from palm oil. Finally, the deposited CHBNC

was washed, vacuum dried at 60°C for 18 h and stored at 4°C. The yield was found to be 88.76%.

High Performance Liquid Chromatography (HPLC)

It is hardly possible to get acemannan in pure form commercially. Therefore, in order to get acemannan in purified form, the gel was processed through number of treatments during isolation and after each treatment; HPLC was carried out on HPLC-UV system. Stationary phase used was the reversed phase C18 column. The active component of the column i.e. adsorbent was octadecyl silane. The mobile phase used was a mixture of 80% water and 20% methanol. In HPLC-UV system, if we click on the peak in the chromatogram we can obtain the UV spectra of the corresponding sample through the special Task Mode of inbuilt LC Chem Station software.

Characterization

Structural characterization

The structural characterization of synthesized CHBNC was carried out by analysing UV-Visible, Fourier Transform Infrared (FTIR), Nuclear Magnetic Resonance (NMR) (¹H, ¹³C and ³¹P) spectra

The UV-Visible spectra were recorded over the 200-600 nm range utilizing the Double R Optics DR-324 C double beam UV-Vis spectrophotometer.

FTIR spectra of chitosan, *Aloe vera* (acemannan), CHC and CHBNC were obtained on Perkin Elmer RX I spectrometer with a resolution and wave number range of 4 cm⁻¹ and 4000-400 cm⁻¹ keeping air as reference.

¹H, ¹³C and ³¹P NMR spectra of chitosan, *Aloe vera* (acemannan) and CHBNC were transcribed on a Bruker AVANCE 600 spectrometer at 600 MHz keeping the working temperature fixed at 25°C. Solvents used were dimethyl sulfoxide for chitosan and CHBNC and deuterium oxide for herbal (*Aloe vera*) (acemannan). Results were analysed in ACD labs software for spectra calibration and peak assignment.

Thermal characterization

The thermal characterization of CHBNC was carried out by Differential Scanning Calorimetry (DSC) (Perkin Elmer, Jade DSC, USA) and Thermo gravimetric Analyzer (TGA) (Perkin Elmer, Pyris 6 TGA, USA). The temperature range was set up from 26 to 445°C for DSC and 26 to 1110°C for TGA under nitrogen atmosphere at a flow rate of 40 ml/min and at a heating rate of 10°C/min.

Surface morphology characterization

Surface morphology characterization was studied using scanning electron microscope (SEM, Zeiss EVO 50) and Atomic Force Microscope (AFM, MFP-3D).

Evaluation of particle size distribution pattern

The measurement of particle size of CHBNC and their distribution pattern in water emulsion were carried out using Brukhaven instrument 90 plus, USA using DLS technique.

Results and Discussion

Synthesis of CHBNC

In solid state, the rigid conformation of long linear chain molecules of chitosan are in tightly folded random coil form. Individual molecular coils are interpenetrating and entangled with each other. In liquid phase, when the extract of herb (*Aloe vera*) gel (acemannan) is added, the liquor gradually diffuses into the chitosan polymer anatomy resulting into the swelling of the polymer with simultaneous formation of chitosan-herbal composite (CHC). As swelling continues, the segments of the resultant polymer are frayed out as bunches of entangled molecules called hydrodynamic sphere, the diameter of which is 3740 nm at 1 g/l concentration. The particle size is minimized to nano level by means of cross linking and electrostatic interactions with STPP. The intermolecular cross linking of chitosan-herbal bionanocomposite (CHBNC) and the chemical reactions involved are shown in Figures 1 and 2. The diameter of nano matrix so formed was found to be 48.73 nm.

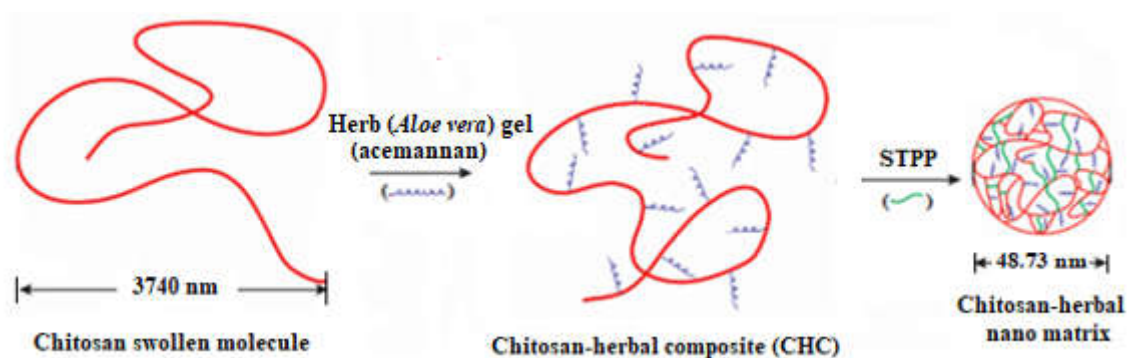
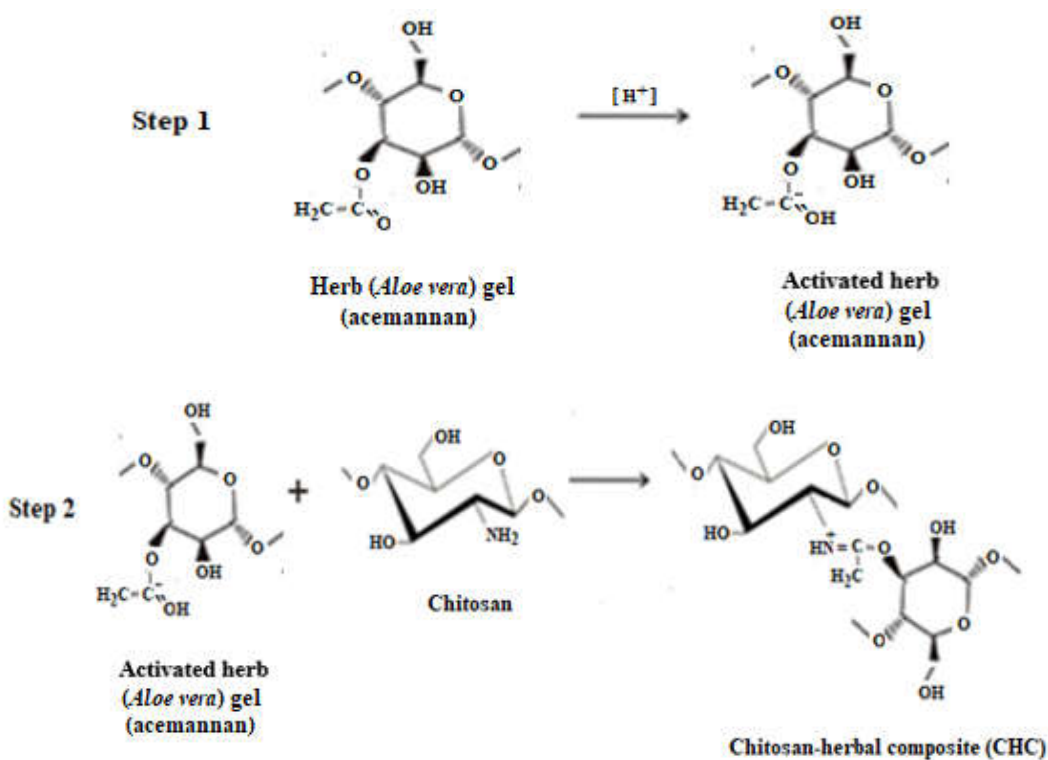


Figure 1. Schematic Structure of Chitosan-Herbal Nano Matrix



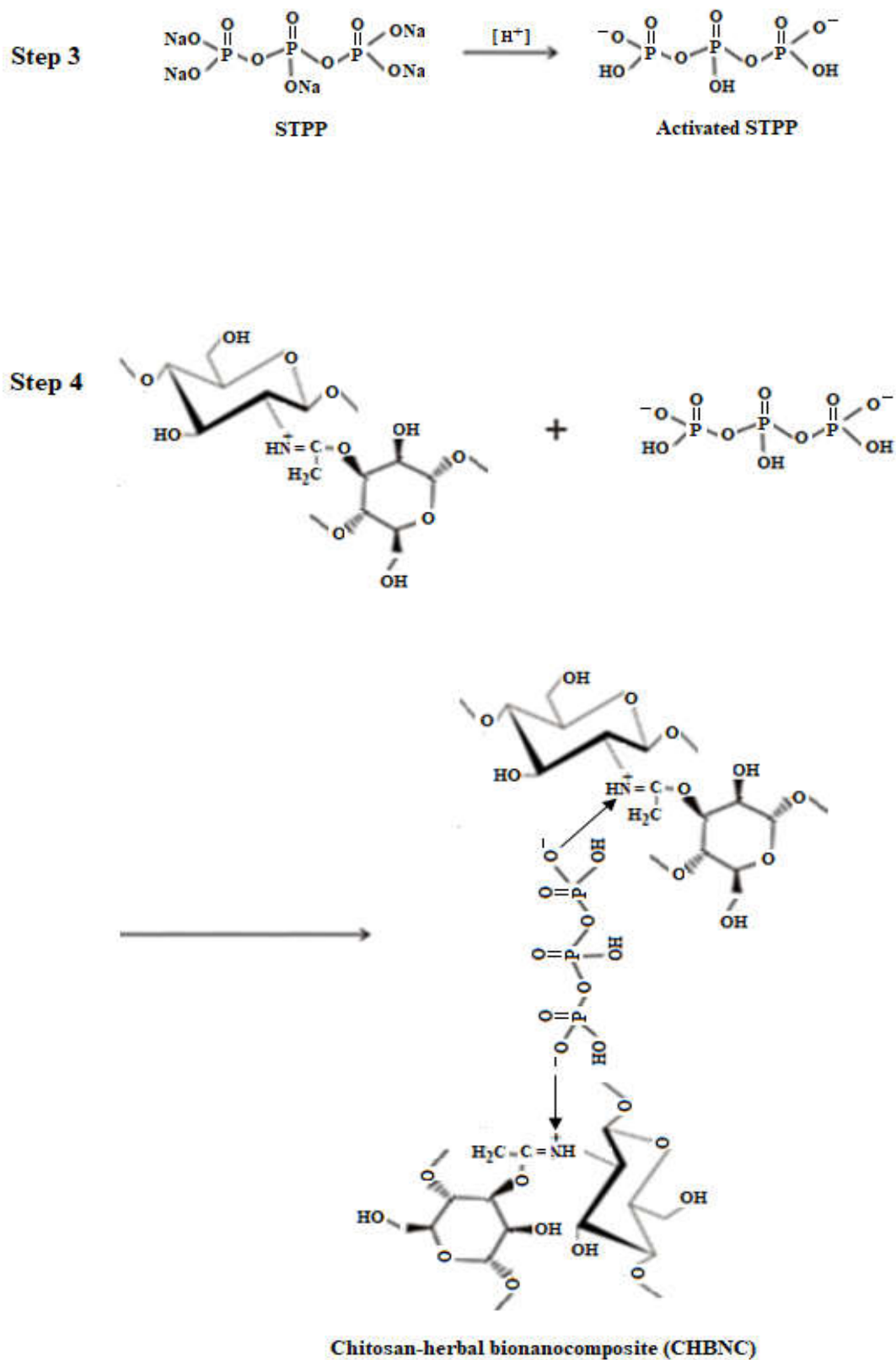
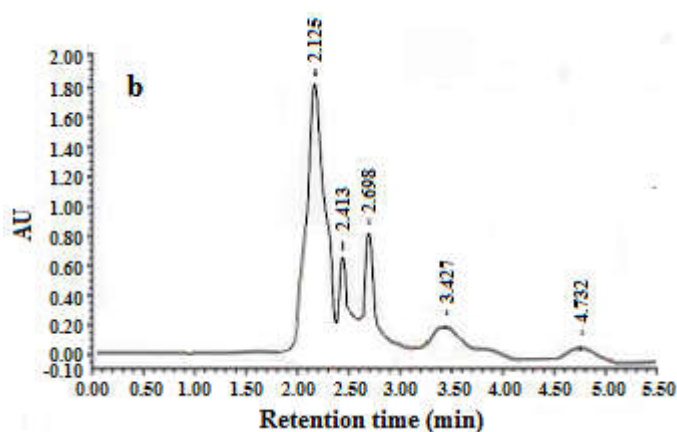
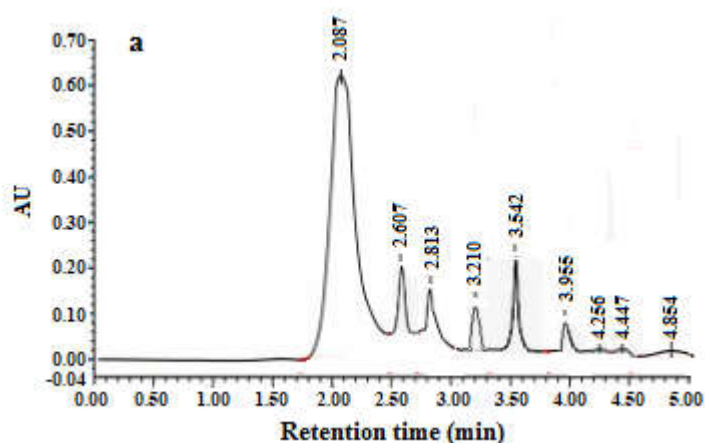


Figure 2. Chemical Reactions Involved for the Production of CHBNC

HPLC chromatogram analysis

Figures 3a, b and c show the HPLC chromatogram of homogenized *Aloe vera* gel, after HCl treatment and after treatment with ethanol. During the process of isolation and purification of acemannan from *Aloe vera* gel, the material obtained at each step (after homogenization *Aloe vera* gel, after HCl treatment and after treatment with ethanol) was analysed by analyzing the HPLC chromatogram recorded. After homogenization of *Aloe vera* gel, the material obtained was analysed with HPLC and the chromatogram so obtained showed a number of peaks against retention time of 2.087, 2.607, 2.813, 3.210, 3.542, 3.955, 4.256, 4.447 and 4.854 min. The identification of constituents was done by comparing the acquired peaks in the spectrum against retention time with the peaks in the reported spectrum [9]. After comparing, it was observed that the peaks shown in Figure 3a are assigned for acemannan, oligosaccharide, monosugars, calcium oxalate, organic acids, magnesium oxalate, calcium lactate, magnesium lactate and anthraquinones. But the number of peaks was found to be reduced down when the material after homogenization was further treated with HCl (Figure 3b). The peaks against retention time 2.125, 2.413, 2.698, 3.427 and 4.732 min so observed were for the presence of acemannan, oligosaccharide, monosugars, organic acids and anthraquinones. When the material was finally treated with 95% ethanol and analysed with HPLC, it gave out only a single peak. The generation of single peak against retention time 2.102 min (Figure 3c) clearly indicates the purity of acemannan. After clicking on the peak in the chromatogram of acemannan we obtained the UV spectra of the corresponding sample having single peak at 270 nm which is also supported by the UV-Visible spectrum of acemannan.



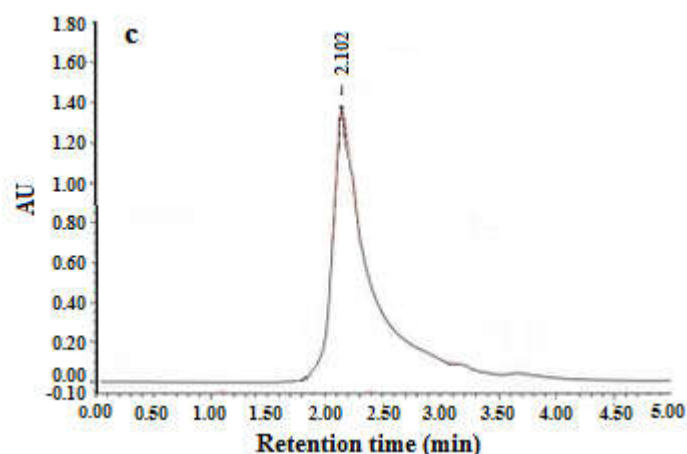


Figure 3. HPLC Chromatogram of a: Homogenized *Aloe vera* Gel, b: Material after Treatment With 10% HCl and c: Material after Treatment with 4 Volumes of 90% Ethanol

UV-Visible spectra analysis

The UV-Visible spectra of chitosan, *Aloe vera* gel extract (acemannan) and CHBNC are shown in Figure 4. In the present study, the absorption peaks noticed at 220 and 270 nm were for the samples of chitosan and *Aloe vera* gel (acemannan). These values are lower than that of the absorption peak of CHBNC (327 nm). According to Kubo theory [10], the absorption band would be blue shifted i.e. shifting of band towards the higher wave length with the decrease of nano particle size. Therefore, CHBNC so formed was nanometric. Moreover, the change of colour of the resultant suspension from off white to pale yellow also indicated the formation of CHBNC.

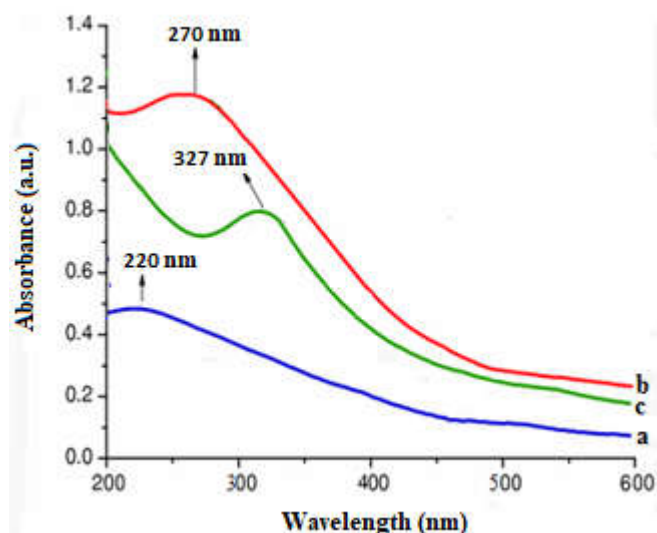


Figure 4. UV-Vis spectra of a: Chitosan, b: *Aloe vera* Gel Extract (Acemannan) and c: CHBNC

Fourier Transform Infrared (FTIR) spectroscopy study

In Figure 5a, chitosan powder shows broad intensity band at 3435.83 cm^{-1} due to overlapping of $-\text{OH}$ and amine $-\text{NH}$ stretching bands. Aliphatic C-H stretching vibration is identified by the presence of a strong peak at 2941.91 cm^{-1} . Further, in the C-H region of FTIR spectrum, the intensity peak at 2898 cm^{-1} is assigned to the asymmetric modes of $-\text{CH}_2$ stretching. Since, the grade of chitosan used in the present study is 81% deacetylated, absorptions are expected due to amide groups. In practice, the peak for $>\text{C}=\text{O}$ stretch of amide bond is observed at 1614.03 cm^{-1} . Strong peaks at 1455.42 cm^{-1} and 1364.76 cm^{-1} showing the presence of $-\text{NH}_2$ stretching and C-H vibration respectively. The peak at 1028.13 cm^{-1} indicates C-O-C glycosidic bond vibrations [11-12] and also corresponds to saccharide structure of chitosan [13].

FTIR spectrum of *Aloe vera* gel (acemannan) is shown in Figure 5b where the appearance of intensity band at 2978.73 cm^{-1} corresponding to the presence of $-\text{CH}$ stretching. The sharp peak at 2896.01 cm^{-1} is attributed to phenolic $-\text{OH}$ stretching. But the main peaks of *Aloe vera* gel (acemannan) are observed against different wave numbers like 1511.78 cm^{-1} , 1455.27 cm^{-1} , 1355.83 cm^{-1} and $436.30 - 448.78\text{ cm}^{-1}$. These are assigned to o-acetyl esters, asymmetrical COO^- stretching, glucan units and C-H vibration [14].

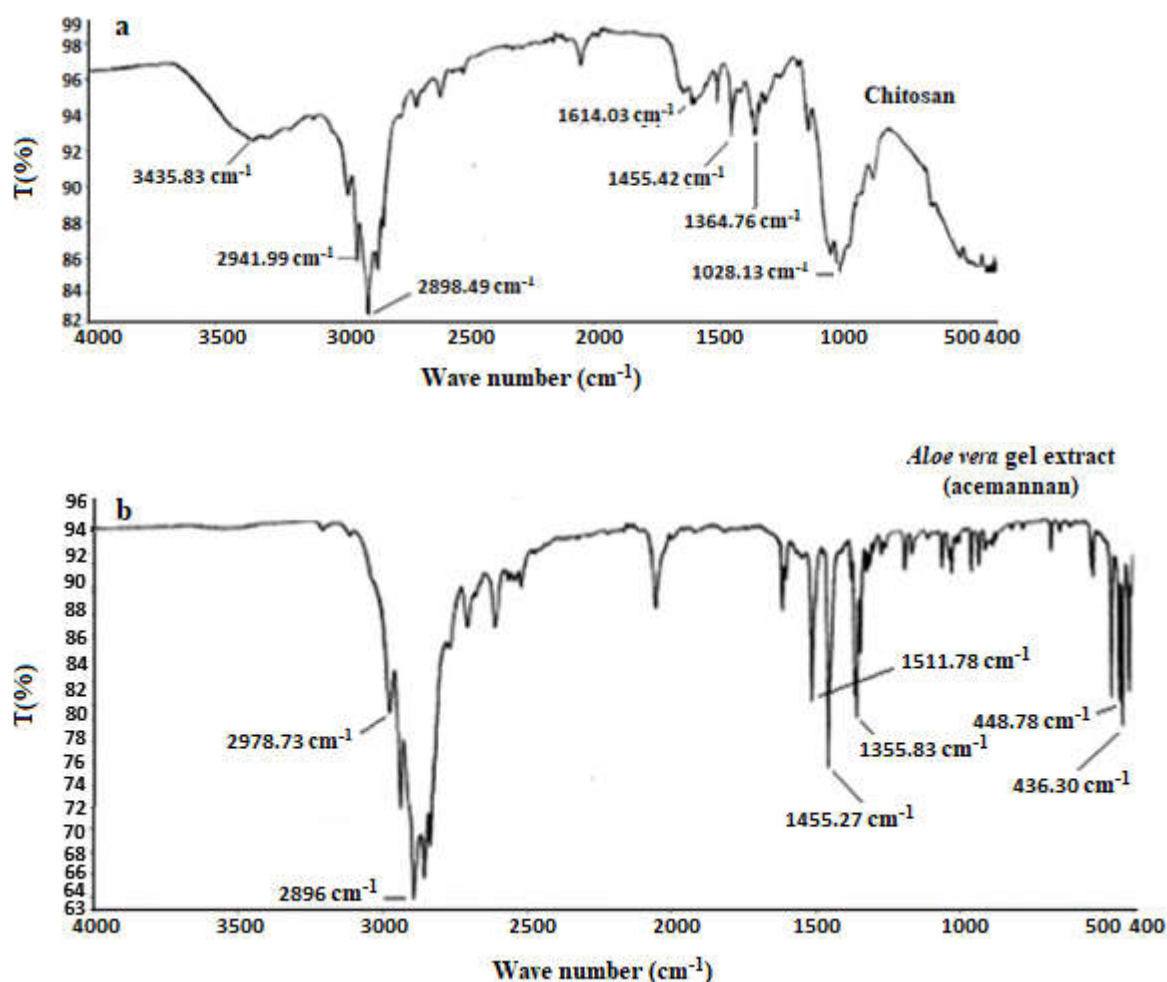


Figure 5. FTIR Spectra of a: Chitosan and b: *Aloe vera* Gel Extract (Acemannan)

In the FTIR spectrum of chitosan-herbal composite (CHC) (as shown in Figure 6a), some differences are visible when compared with the spectrum of chitosan and herb (*Aloe vera*) gel (acemannan). The absorption band at 1614.03 cm^{-1} , 1455.42 cm^{-1} and 1364.76 cm^{-1} found in chitosan spectrum shifted to 1512.21 cm^{-1} , 1455.51 cm^{-1} and 1356.29 cm^{-1} and become sharper and longer in the chitosan-herbal composite spectrum indicating the formation of bond between the $-\text{NH}_2$ of chitosan and the acetyl group of acemannan. The FTIR spectrum of STPP is shown in Figure 6b. The appearance of peaks against different wave numbers viz. 1126.14 cm^{-1} , 885.09 cm^{-1} and 473.73 cm^{-1} indicate the presence of P=O, P-O-P and O-P-O stretching respectively.

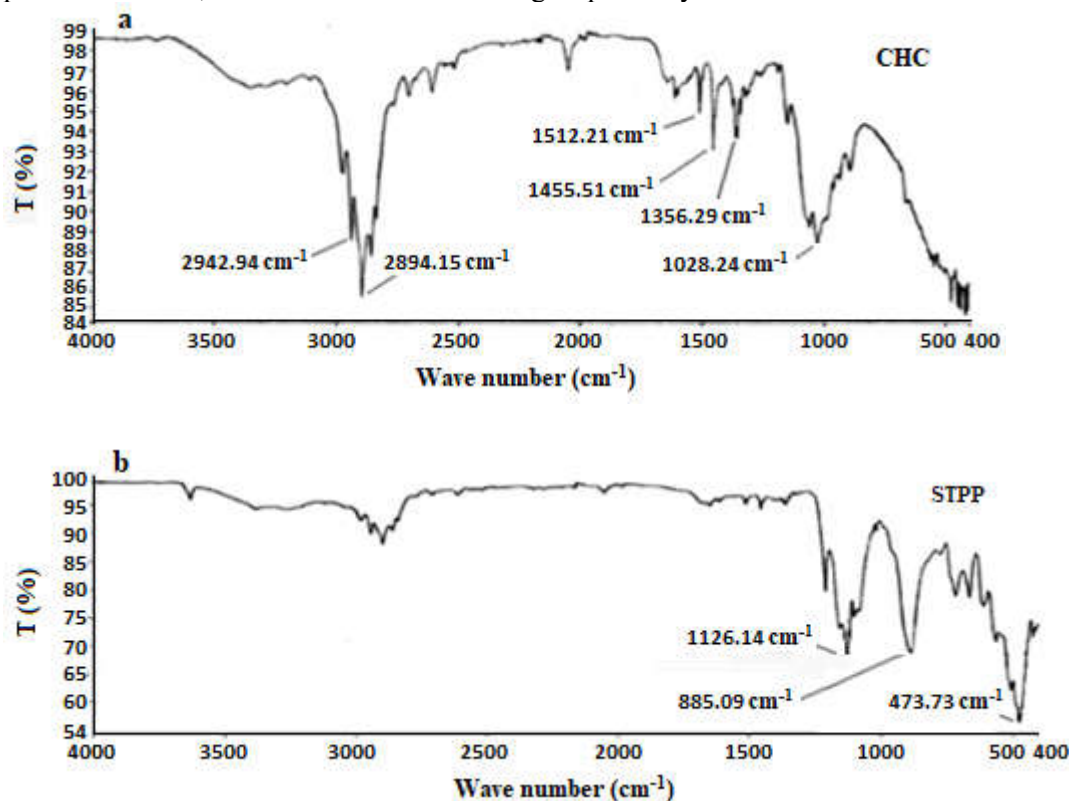


Figure 6. FTIR Spectra of a: CHC and b: STPP

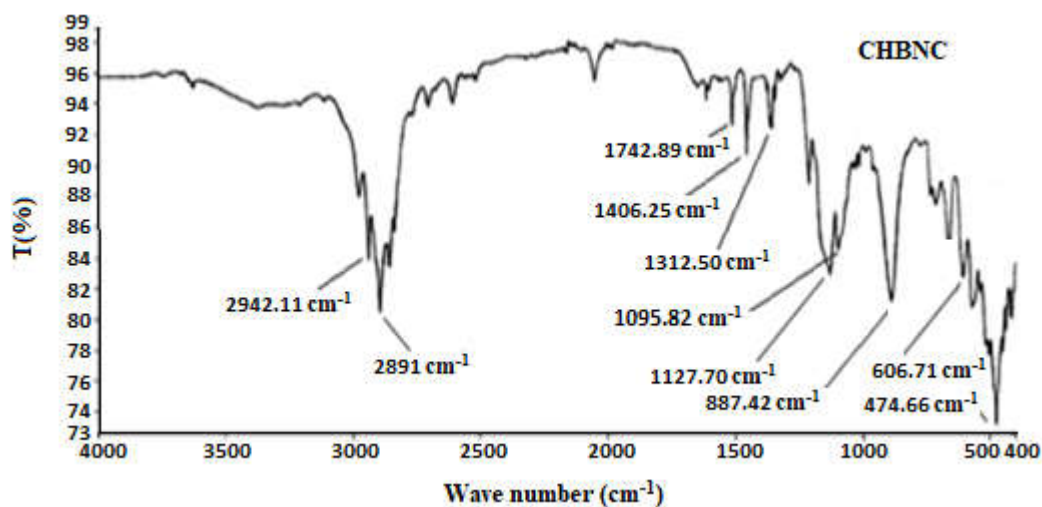


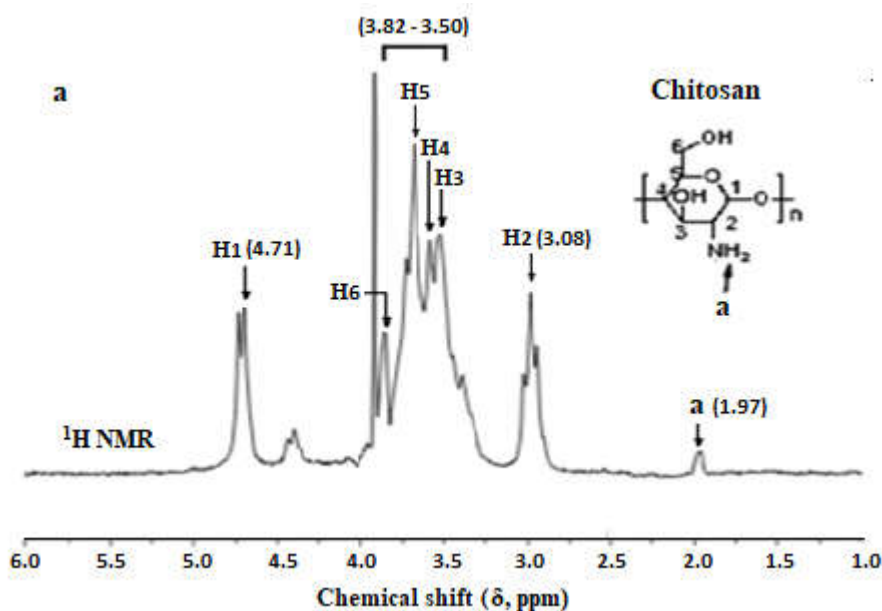
Figure 7. FTIR Spectra of CHBNC

In the FTIR spectrum of CHBNC (as shown in Figure 7), the decrease and shifting of peaks from 1512.21 cm^{-1} to 1472.89 cm^{-1} , 1455.51 cm^{-1} to 1406.25 cm^{-1} and 1356.29 cm^{-1} to 1312.50 cm^{-1} are observed with the formation of sharp peaks in the regions 1127.7 cm^{-1} , 1095.82 cm^{-1} and 887.42 cm^{-1} demonstrating the formation of nanocomposite between chitosan and herb (*Aloe vera*) gel (acemannan) cross linked with STPP. Moreover, the decrease in the intensity of peak at 1406.25 cm^{-1} indicates the minimization of free $-\text{NH}_2$ groups which is an indication of the binding of herb (*Aloe vera*) gel (acemannan) with the amide group ($-\text{NH}_2$) of chitosan, crosslinking of P-O^- groups of STPP with the $-\text{NH}^+$ of chitosan and formation of $\text{CH}_2-\text{NH}^+ \leftarrow \text{O-P}$ [15]. This is also supported by the presence of peaks of STPP at 1127.70 cm^{-1} , 887.42 cm^{-1} and 474.66 cm^{-1} in the CHBNC spectrum.

Nuclear Magnetic Resonance (NMR) study

Figure 8a shows the ^1H NMR spectrum of chitosan where chemical shift (δ) = 4.71, (δ) = 3.08 and $\delta = 3.50\text{-}3.82$ are assigned to protons associated with H_1 , H_2 and $\text{H}_3\text{-H}_6$ positions of chitosan. Another signal at lower chemical shift ($\delta = 1.97$) reflects the presence of $-\text{NH}_2$ group in chitosan structure (represented as a in Figure 8a).

The ^{13}C NMR of chitosan is shown in Figure 8b where the appearance of signal at 104.4 ppm attributes to C_1 carbon of chitosan. The signals at various chemical shifts such as 60 ppm, 75 ppm, 83 ppm, 79 ppm and 65 ppm indicate the presence of C_2 , C_3 , C_4 , C_5 and C_6 carbons of chitosan respectively. A signal is also observed at 28 ppm which is due to the presence of $-\text{NH}_2$ group in chitosan structure.



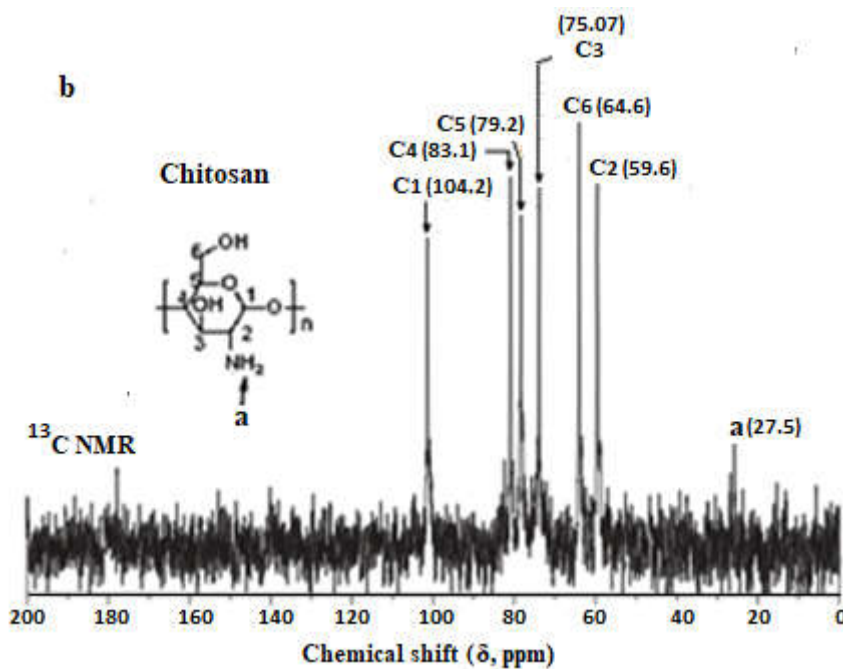
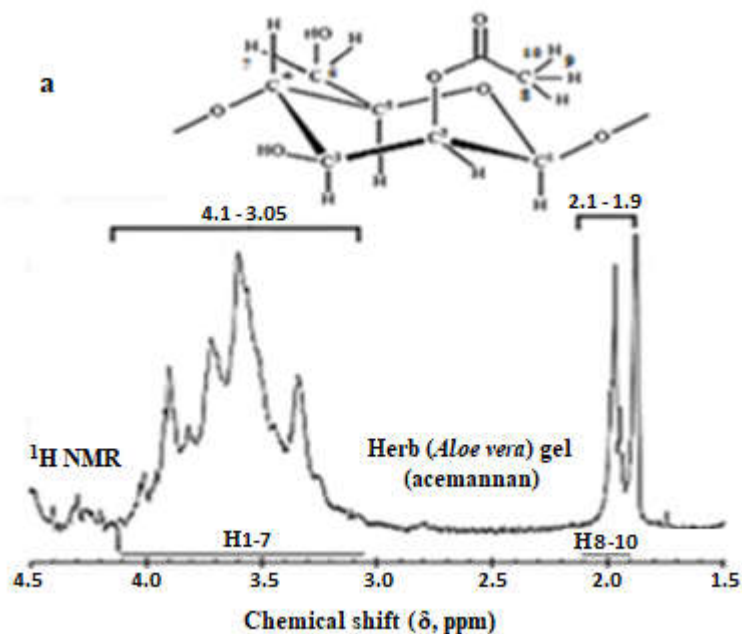


Figure 8. Spectra of (a) ¹H NMR and (b) ¹³C NMR of Chitosan

In the ¹H NMR spectrum of *Aloe vera* gel (acemannan) (as shown in Figure 9a) protons on the acetyl group occurs at chemical shift 1.9 – 2.1 ppm while protons on the glucan unit at C₁ – C₆ (H₁ – H₇) occurs at δ = 3.05 – 4.1 ppm.

The ¹³C NMR spectrum of *Aloe vera* gel (acemannan) (as shown in Figure 9b) shows signal at δ = 102.43 ppm, 90.3 ppm, 89.1 ppm, 86.42 ppm, 82.3 ppm, 80.72 ppm, 72.52 ppm and 69.25 ppm which are assigned to C₁, C₄, C₅, C₆, C₇, C₂, C₃ and C₈ carbons of acemannan structure respectively.



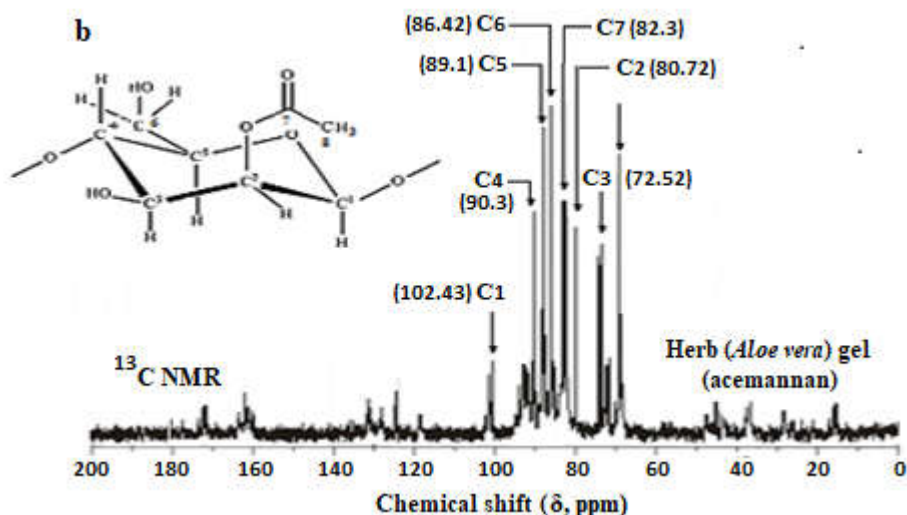
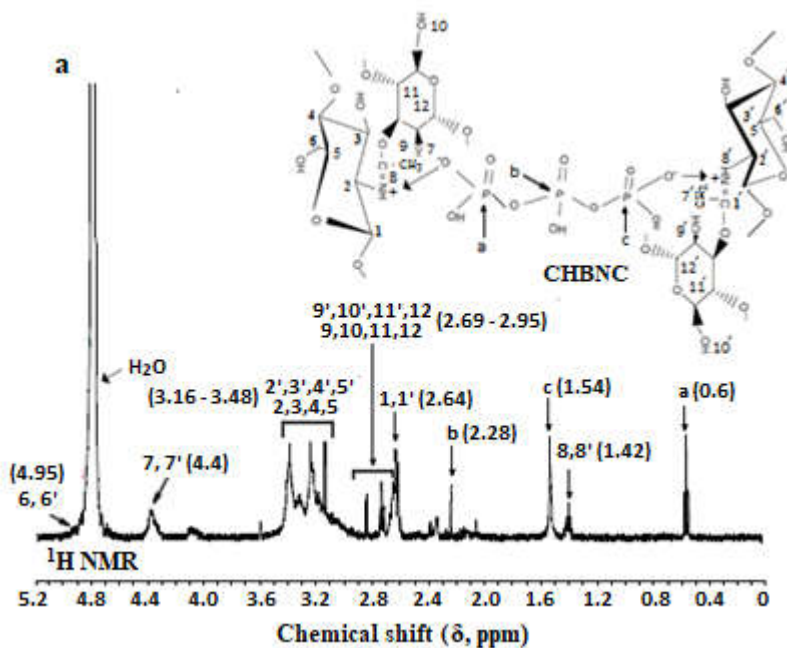


Figure 9. Spectra of (a) ¹H NMR and (b) ¹³C NMR of Herb (*Aloe vera*) Gel

Figure 10a shows the ¹H NMR of CABNC where (δ) = 2.64, (δ) = 3.16 – 3.48, δ = 4.95 and δ = 1.42 ppm are assigned to protons associated with 1, 1' – 6, 6' positions and amide group of chitosan chain. The signals of protons of 1 – 6 positions are overlapped with the signals of protons of 1' – 6' positions of chitosan chain. The signals at (δ) = 4.4 and (δ) = 2.69 – 2.95 ppm are assigned to protons associated with 7, 7' and 9, 9' – 12, 12' positions of attached acemannan structure of *Aloe vera* gel whereas (δ) = 0.6, (δ) = 2.28 and (δ) = 1.54 ppm are assigned to the presence of three phosphorus elements in the main chain of STPP which is present in the CHBNC in cross linked form.



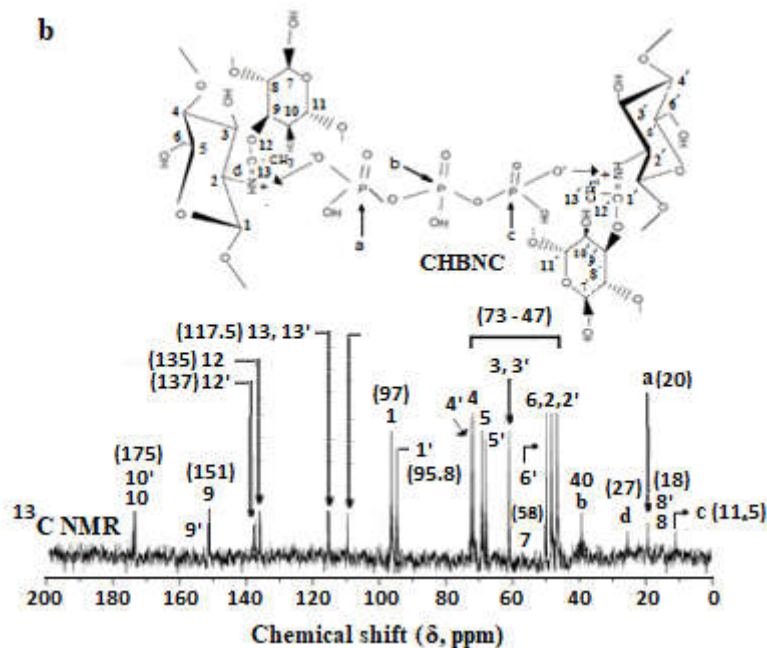


Figure 10. Spectra of (a) ¹H NMR and (b) ¹³C NMR of CHBNC

In ¹³C NMR of CHBNC (as shown in Figure 10b), the signals at (δ) = 97 ppm and (δ) = 47 – 73 ppm are assigned to carbons associated with 1, 1' and 2, 2' – 6, 6' positions of chitosan chain. Again, the signals showing at (δ) = 58, (δ) = 18, (δ) = 151, (δ) = 175, (δ) = 110, (δ) = 135, (δ) = 137 and (δ) = 117.5 ppm are assigned to the carbons present in different positions like 7, 7' – 13, 13' of acemannan of *Aloe vera* gel. The signals assigned at (δ) = 20, (δ) = 40 and (δ) = 11.5 ppm represents three phosphorus elements (represented as a, b and c in Figure 10a) in STPP which has been cross linked with chitosan-*Aloe vera* composite by forming a bond between chitosan-*Aloe vera* –NH⁺ and –O–P of STPP. The formation of signal at (δ) = 27 ppm (represented as d in Figure 10b) clearly supports the statement.

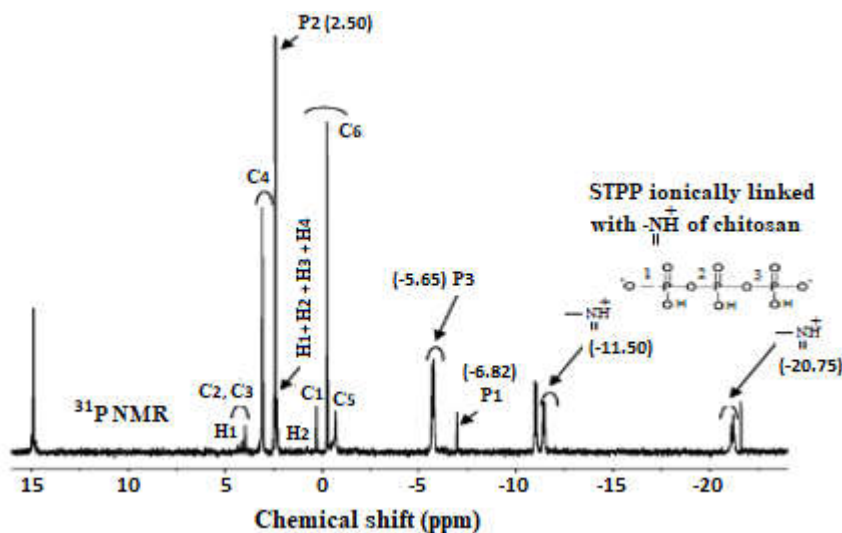


Figure 11. ³¹P NMR Spectrum of CHBNC

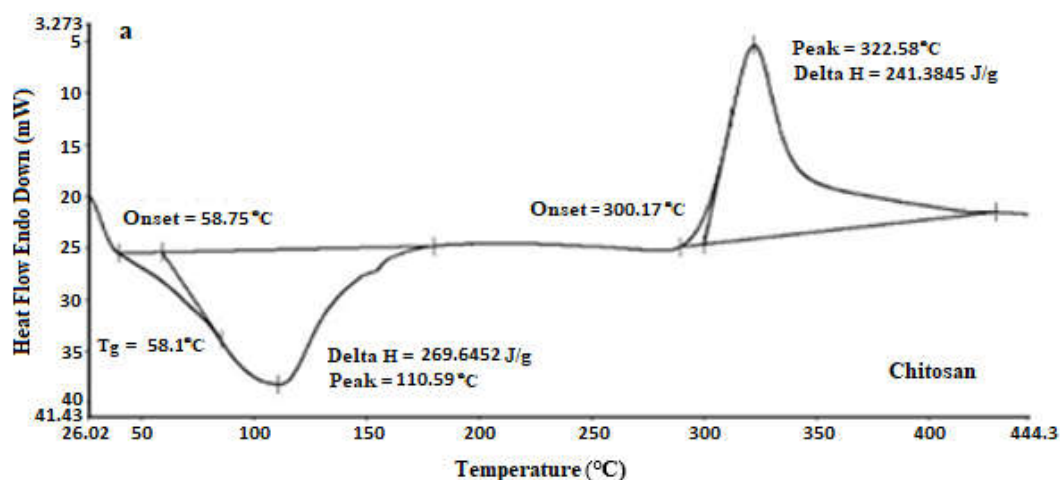
In order to confirm the cross linking of STPP with chitosan *Aloe vera* composite and formation of CHBNC, ^{31}P NMR of CHBNC has been carried out. Figure 11 shows the ^{31}P NMR spectrum of CHBNC. The results indicate that CHBNC contain TPP and attached to the $-\text{NH}^+$ of chitosan-*Aloe vera* composite as ionic linkage which is clearly visible from the two sharp peaks at -11.50 and -20.75 ppm. The signals at -6.82 ppm, 2.5 ppm and -5.65 ppm correspond to three phosphorus elements present in the structure of STPP. Apart from this, a total shift of carbon ($\text{C}_1 - \text{C}_6$) and hydrogen ($\text{H}_1 - \text{H}_6$) of chitosan ring is observed due to the ionic linkages between chitosan-*Aloe vera* and STPP.

Differential Scanning Calorimetry (DSC) studies

Differential Scanning Calorimetry (DSC) monitors heating effects associated with phase transitions and chemical reactions as a function of time. So, for evaluating phase transition of CHBNC, melting point and interaction/complexion of chitosan with *Aloe vera*, DSC analysis was performed on chitosan, *Aloe vera* gel (acemannan) and CHBNC.

The DSC thermogram of chitosan is shown in Figure 12a. Chitosan exhibited a broad endothermic peak centered at about 110.59°C . This peak is attributed to the loss of water associated with the hydrophilic groups ($-\text{OH}$) of chitosan polymer. This suggests that the supplied sample was not completely anhydrous and some bound water was still not removed when dried in the desiccators, which is confirmed by the results obtained from TGA. The sharp exothermic peak which appears at 322.58°C corresponds to the decomposition of polymeric chain molecules of chitosan. The glass transition temperature (T_g) of chitosan polymer is observed at 58.1°C . The endothermic peak at 110.59°C followed by exothermic peak at 322.58°C showing the crystallization and melting process of polymers at different temperatures. This is in accordance with the findings of Al-Masry et al. [16].

The DSC thermogram detail of *Aloe vera* gel (acemannan) is shown in Figure 12b. A sharp peak obtained at 120.17°C is due to the removal of the absorbed water and a blunt exothermic peak at 337.43°C is associated with the breakage of saccharide ring and the bond rupture of linked groups. The glass transition temperature (T_g) is found to be 49°C . The lower ΔH (0.7885 J/g) of *Aloe vera* gel indicates lesser portion of ordered structure of acemannan resulting in higher mobility of acemannan molecules, plausibly owing to the less crystallinity behaviour of *Aloe vera* gel. With lower ordered structure in acemannan of *Aloe vera* gel, acemannan molecules can move with more ease, resulting in lower T_g [17].



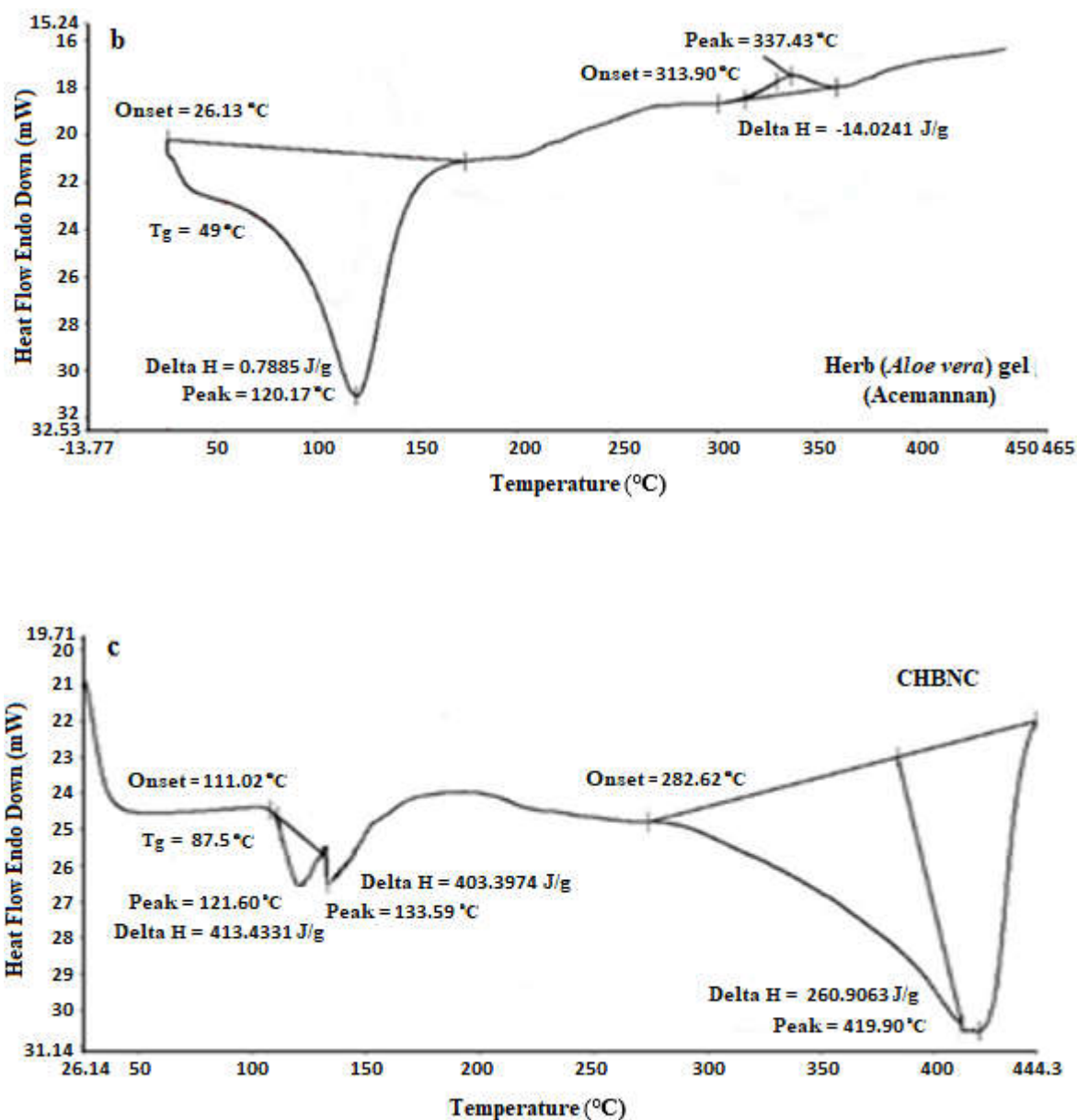


Figure 12. DSC thermogram of a: chitosan, b: *Aloe vera* gel (acemannan) and c: CHBNC

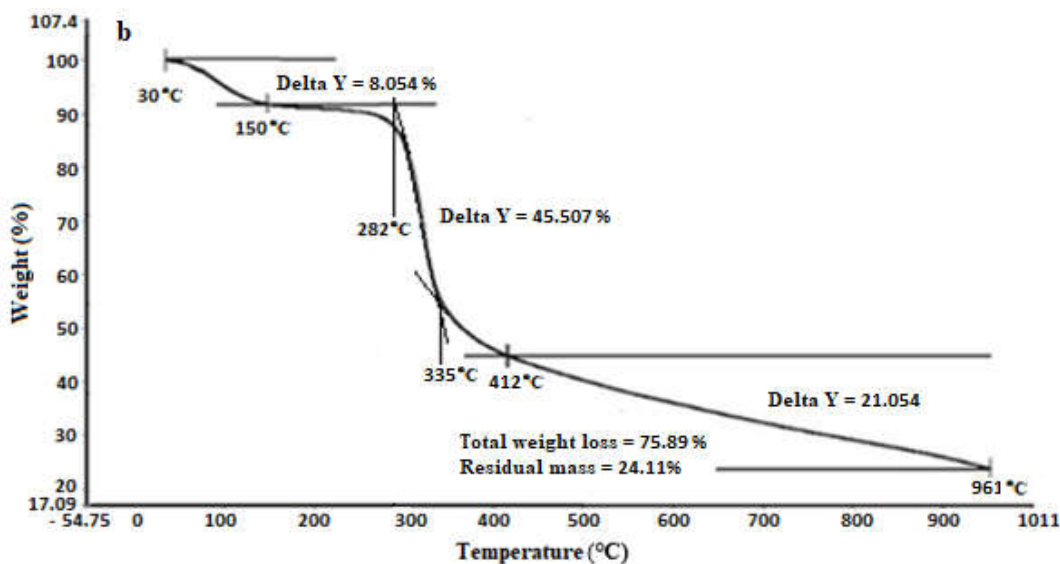
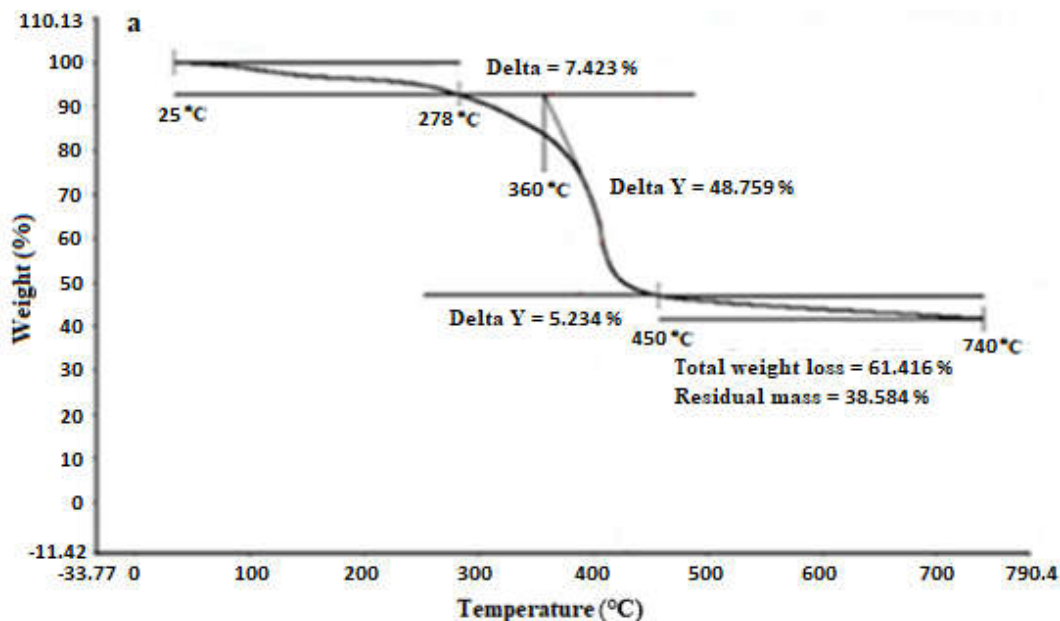
Figure 12c represents the DSC thermogram detail of CHBNC. Two close exothermic peaks are observed at 120.60°C and 133.59°C. These are due to the concurrent phenomena of melting and recrystallization followed by the initiation of final melting [18]. Another broad endothermic peak at 419.90°C is associated with the breakage of cross linkages, delinking of acemannan from chitosan polymer chain molecules and decomposition of acemannan ring and chitosan chains [19]. The glass transition temperature (T_g) is found to be 87.5°C. The higher delta H (413.4331 J/g) of CHBNC indicates larger portion of ordered structure of CHBNC resulting in lower mobility of chain molecules of CHBNC due to its comparatively more crystallinity behaviour with the higher ordered structure in CHBNC, CHBNC cannot move with more ease, resulting in higher T_g [20].

The observation of single T_g in the DSC heating curves indicates that chitosan, *Aloe vera* and STPP are highly compatible. The higher onset temperatures are associated with higher thermal stability. From the obtained higher onset temperature and higher value of T_g it is concluded that CHBNC is found to be highly thermally stable [21].

Thermogravimetric analysis (TGA)

Thermogravimetric analysis (TGA) is a method of thermal analysis in which changes in physical and chemical properties of materials are measured as a function of increasing temperature (with constant heating rate), or as a function of time (with constant temperature and/or constant mass loss).

Thermogravimetric analysis (TGA) is conducted on an instrument referred to as a thermogravimetric analyzer.



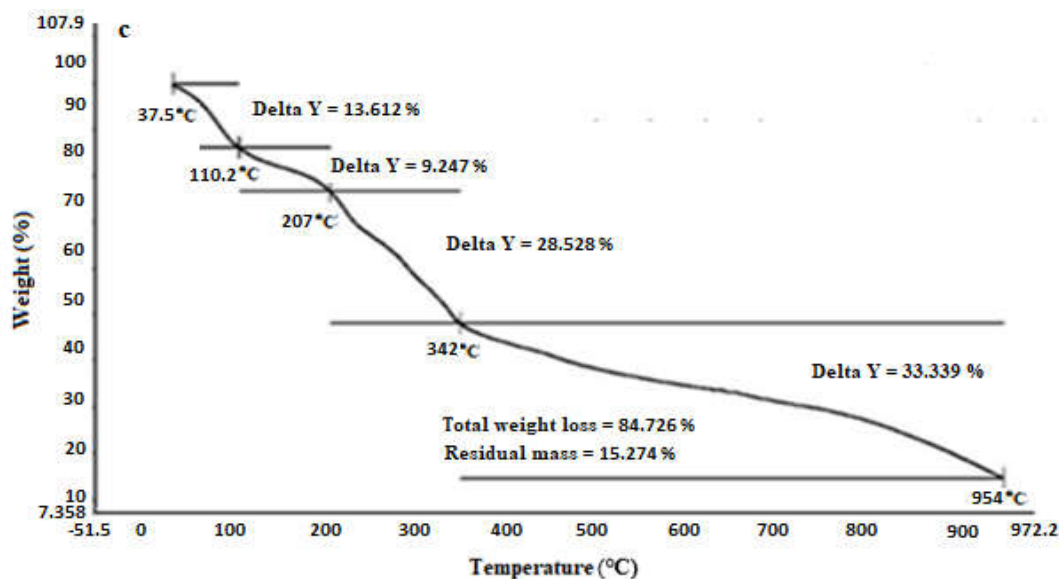


Figure 13. TGA thermogram of a: chitosan, b: *Aloe vera* gel (acemannan) and c: CHBNC

The TGA thermogram of chitosan (as shown in Figure 13a) shows three steps of degradation. Initial degradation occurs at around 30-150°C with 8.054% weight loss which may correspond to a loss of adsorbed/bound water/moisture due to vaporization [22]. The above decomposition for chitosan can also be attributed to the strong water adsorptive nature of chitosan. The second stage of degradation initiates at 150°C, picks up its acceleration at 282°C and continues up to 412°C. There is 46.807% weight loss occurring in the second stage due to degradation of chitosan biopolymer and the temperature at which maximum degradation takes place is found to be 335°C. For the third stage, 21.084% weight loss is observed over a temperature ranging from 412 - 961°C which is mostly associated with the degradation of polymer fragments. At the end of 961°C, the total weight loss is found to be 75.89% and the amount of sample remained as residue at the end of experiment is observed to be 24.11%.

Four main weight loss stages are observed in the TGA thermogram of *Aloe vera* gel (acemannan) (Figure 13b). The first stage weight loss (13.642%) is observed over the temperature ranging from 37.5 - 110.2°C, mostly associated with the loss of free and bound water adsorbed in the structural network [23]. The second stage weight loss (9.247%) appears over the temperature ranging from 110.2 - 207°C. This is most likely due to the degradation or decomposition of lower molecular weight proteins/polysaccharide components, glycerol compounds along with evaporation of structurally bound water in the substrate network. The third stage of degradation occurs at around 207 - 342°C with 28.568% weight loss which is mostly associated with the thermal degradation of acemannan of *Aloe vera* gel [24]. The fourth stage of degradation occurs at 342°C and continues upto 954°C with a weight loss of 33.339%. This may be associated with the carbonization of acemannan [25]. At the end of 954°C, the total weight loss of *Aloe vera* gel (acemannan) is found to be 84.796 with a residual mass of 15.27%.

The TGA thermogram of CHBNC is shown in Figure 13c. For CHBNC, the first stage weight loss (7.403%) is observed over the temperature ranging from 25 - 278°C. This is due to elimination of water bound to the polar groups in chitosan and polysaccharides (acemannan) of *Aloe vera* gel [26]. The second stage weight loss (48.759%) at around 278 - 450°C corresponds to the thermal decomposition of polymer matrix of CHBNC and the temperature at which maximum decomposition observed is 360°C. The third stage weight loss (5.236%) is observed over the temperature ranging from 450 - 740°C which is mostly

associated with the depolymerisation of polymeric chain, rupture of chemical bonds and finally carbonization of the fragments of the depolymerized chain of chitosan, polysaccharides rings and STPP. At the end of experiment, the total weight loss is found to be 61.398% indicating that 38.602% of the CHBNC remained as residue.

SEM and AFM studies

The topography, morphologies and forms of materials are examined with the help of SEM and AFM. Under SEM and AFM examination, chitosan reveals flaky, nonporous, smooth and even surface structure with plain texture as shown in Figures 14a and 15a. The morphology of *Aloe vera* gel (acemannan) in powder form mostly appears to be porous and spongy (Figures 14b and 15b) whereas SEM and AFM images of CHBNC (Figures 14c and 15c) show an uneven surface morphology and roughness with higher compactness as compared to Chitosan and *Aloe vera* gel (acemannan) alone.

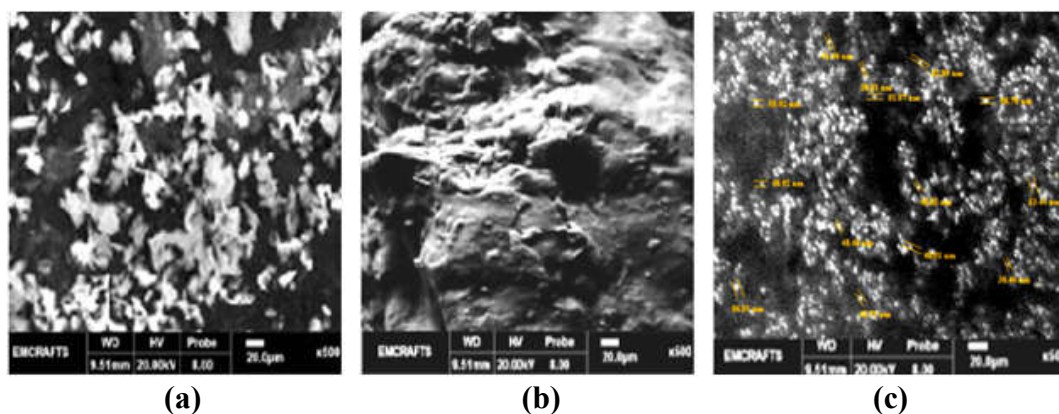


Figure 14. SEM micrograph of a: chitosan, b: *Aloe vera* gel (acemannan) and c: CHBNC

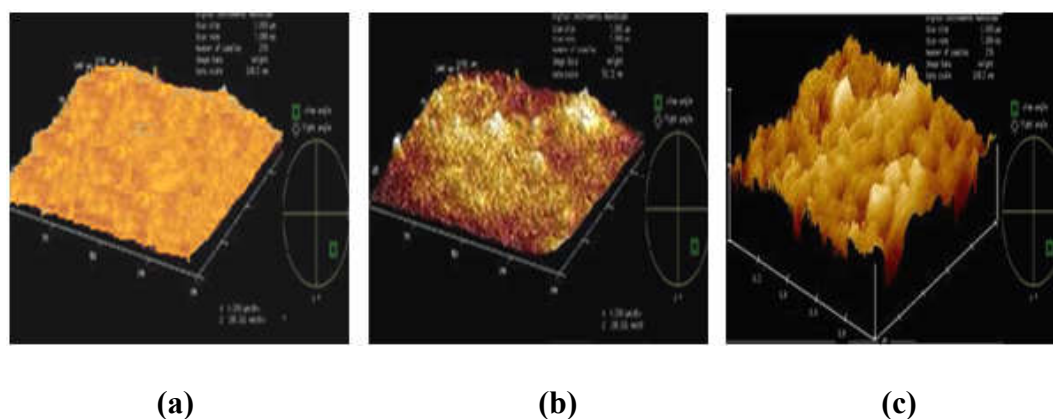


Figure 15. AFM micrograph of a: chitosan, b: *Aloe vera* gel (acemannan) and c: CHBNC

Particle size and their distribution pattern in the emulsion of CHBNC

In order to evaluate the particle size distribution pattern of CHBNC in aqueous phase, it was mixed with a solution of phosphate buffer (pH 7) with continuous stirring for 20 min. The colour of the resultant solution was observed as pale yellow which turned into a clear colourless solution after a span of 5 min. This is due to the “Plasmon resonance” within the generated nano particles of CHBNC in phosphate buffer solution. Again, the initial optical density of the emulsion was found to be 0.68 which decreased significantly to the level of 0.31 after completion of emulsification process. This also confirms the generation of nano particles of CHBNC in its emulsion as optical properties of nano particles within the emulsion are very much its shape and size dependent [27]. The particles were found to be nearly spherical in shape with diameter ranging from 10.05 nm to 87.46 nm (Figure 16) which ultimately showed the average particle diameter as 48.73 nm.

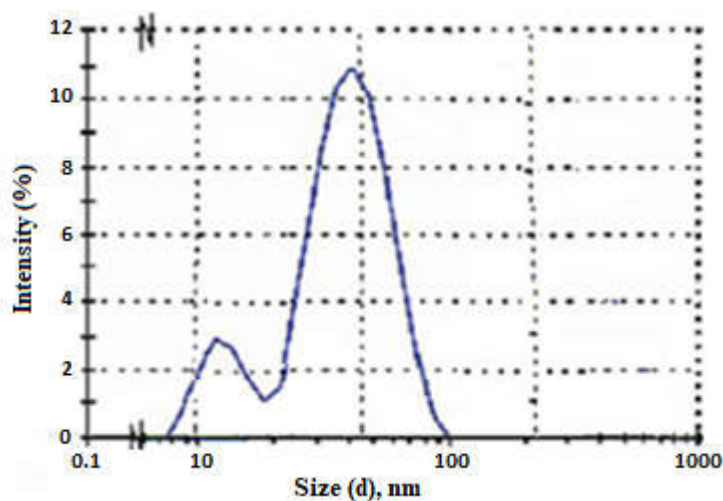


Figure 16. Particle size distribution pattern of CHBNC in water emulsion

Conclusion

Chitosan-herbal bionanocomposite (CHBNC) has been synthesized successfully with an average nanometric diameter of about 48.73 nm. The blue shift of wave length to the higher order and colour change during CHBNC formation confirms the formation of its nano matrix. The structural characterization of CHBNC was performed through UV-Visible, FTIR, ^1H , ^{13}C and ^{31}P NMR spectra. The analysis of peaks observed in the finger print regions of different spectra confirms the interaction between chitosan, herb (*Aloe vera*) gel (acemannan) and STPP within the nano structure of the synthesized CHBNC. The DSC and TGA studies clearly indicate the high thermal stability of CHBNC with rough surface morphology as identified from SEM and AFM micrographs.

References

- [1] Q. Li, Z. Xue, Y. Wu and X. Zeng, “The Status of Quo and Prospect of Sustainable Development of Smart Clothing”, *Sustainability*, vol. 14, no. 2, (2022), p. 990.
- [2] M. Naebe, A. N. M. A. Haque and A. Haji, “Plasma Assisted Antimicrobial Finishing of Textiles: A Review”, *Engineering*, vol. 12, (2022), pp. 145-163.

- [3] F. Tanasa, C-A. Teaca, M. Nechifor, M. Ignat, I. A. Duceac and L. Ignat, “Highly Specialized Textiles with Antimicrobial Functionality-Advances and Challenges”, *Textiles*, vol. 3, no.2, (2023), pp.219-245.
- [4] M. Karypidis, E. Karanikas, A. Papadaki and E. G. Andriotis, “A Mini-Review of Synthetic Organic and Nanoparticle Antimicrobial agents for Coating in Textile Applications”, *Coatings*, vol. 13, no. 4, (2023), p. 693.
- [5] R. Gulati, S. Sharma and R. K. Sharma, “Antimicrobial Textile: Recent Developments and Functional Perspective”, *Polymer Bulletin*, vol. 79, no. 8, (2022), pp. 5747-5771.
- [6] A. Elamri, K. Zdiri, M. Hamdaoui and O. Harzallah, “Chitosan: A Biopolymer for Textile Processes and Products”, *Textile Research Journal*, vol. 93, no. 5-6, (2023), pp. 1456-1484.
- [7] C-L. Ke, F-S. Deng, C-Y. Chuang and C. H. Lin, “Antimicrobial Action and Application of Chitosan”, *Polymers*, vol. 13, no. 6, (2021), p. 904.
- [8] Y. Bai, Y. Niu, S. Pin and Ma, G, “A New Biomaterial Derived from *Aloe vera* – Acemannan from Basic Studies to Clinical Application”, *Pharmaceutics*, vol. 15, no. 7, (2023), p.1913.
- [9] C. Liu, Y. Cui, F. Pi, Y. Cheng, Y. Guo and H. Qian, “Extraction, Purification, Structural Characteristics, Biological Activities and Pharmacological Applications of Acemannan, A Polysaccharide from *Aloe-vera*: A Review”, *Molecules*, vol. 24, no. 8, (2019), p. 1554.
- [10] R. Kubo, “Statistical-Mechanical Theory of Irreversible Processes. I. General Theory and Simple Applications to Magnetic and Conduction Problems”, *Journal of the Physical Society of Japan*, vol. 12, no. 6, (1957), pp. 570-586.
- [11] A. Poerio, T. Girardet, C. Petit, S. Fleutot, J-P. Jehl, E. Arab-Tehrany, J. F. Mano and F. Cleymand, “Comparison of the Physicochemical Properties of Chitin Extracted from *Cicada orni* Sloughs Harvested in Three Different Years and Characterization of the Resulting Chitosan”, *Applied Sciences*, vol. 11, no. 23, (2021), p. 11278.
- [12] M. Triunfo, E. Tafi, A. Guarnicri, R. Salvia, C. Scieuzo, T. Hahn, S. Zibek, A. Gagliardini, L. Panariello, M. B. Coltelli, A. D. Bonis and P. Falabella, “Characterization of Chitin and Chitosan Derived from *Hermetia illucens* , A Further Step in A Circular Economy Process”, *Scientific Reports*, vol. 12, (2022), p.6613.
- [13] F. Momtaz, E. Momtaz, M. A. Mehrgardi, M. Momtaz, T. Narimani and F. Poursina, “Enhanced Antibacterial Properties of Polyvinyl Alcohol/Starch/Chitosan Films with NiO-CuO Nanoparticles For Food Packaging”, *Scientific Reports*, vol. 14, (2024), p. 7356.
- [14] S. T. L. Jales, R. M. Barbosa, A. C. deAlbuquerque, L. H. V. Duarte, G. R. daSilva, L. M. A. Meirelles, T. M. S. daSilva, A. F. Alves, C. Viseras, F. N. Raffin and F. A. deMoura, “Development and Characterization of *Aloe vera* Mucilaginous-Based Hydrogels for Psoriasis Treatment, *Journal of Composite Science*, vol. 6, no. 8, (2022), p. 231.
- [15] S. Samadieh and M. Sadri, “Preparation and Biomedical Properties of Transparent Chitosan/gelatin/Honey./*Aloe vera* Nanocomposite, *Nanomedicine Research Journal*, vol. 5, no. 1, (2020), pp. 1-12.
- [16] W. A. Al-Masry, S. Haider, A. Mahmood, M. Khan, S. F. Adil and M. R. H. Siddiqui, “Evaluation of the Thermal and Morphological Properties of γ -Irradiated Chitosan-Glycerol-Based Polymeric Films”, *Processes*, vol. 9, no. 10, (2021), p. 1783.
- [17] M. Sanchez, E. Gonzalez-Burgos, I. Iglesias and M. P. Gómez-Serranillos, “Pharmacological Update Properties of *Aloe vera* and Its Major Active Constituents”, *Molecules*, vol. 25, no. 6, (2020), p. 1324.
- [18] M. Naffakh and P. S. Shuttleworth, “Investigation of the Crystallization Kinetics and Melting Behaviour of Polymer Blend Nanocomposites Based on Poly (L-Lactic Acid), Nylon 11 and TMDCs WS₂”, *Polymers*, vol. 14, no. 13, (2022), p. 2692.
- [19] A. Piotrowska-Kirschling and J. Brzeska, “The Effect of Chitosan on the Chemical Structure, Morphology and Selected Properties of Polyurethane/Chitosan Composites”, *Polymers*, vol. 12, no. 5, (2020), p. 1205.

- [20] Y. Huang, S. Hao, J. Chen, M. Wang, Z. Lin and Y. Liu, "Synthesis and Characterization of a novel Chitosan-Based Nanoparticle-Hydrogel Composite System Promising For Skin Wound Drug Delivery", *Marine Drugs*, vol. 22, no. 9, (2024), p. 428.
- [21] C. Chen, W. Liang, F. Fan and C. Wang, "The Effect of Temperature on the Properties of Hydrochars Obtained by Hydrothermal Carbonization of Waste *Camellia oleifera* Shells", *ACS Omega*, vol. 6, no. 25, (2021), pp. 16546-16552.
- [22] S. F. Hamza, M. M. El-Sawy, N. A. Alian and N. O. Shaker, "Synthesis and Evaluation of Performance Characteristics Green Composites from Sustainable Fatty Chitosan Graft Copolymer with Acrylic Acid for Waste Water Treatment", *Egyptian Journal of Chemistry*, vol. 64, no. 10, (2021), pp. 6007-6015.
- [23] M. C. Otálora, A. Wilches-Torres and J. A. G. Castaño, "Extraction and Physicochemical Characterization of Dried Powder Mucilage from *Opuntia ficus-indica* Cladodes and *Aloe vera* leaves: A Comparative Study", *Polymers*, vol. 13, no. 11, (2021), p. 1689.
- [24] M. Chelu, M. Popa, E. A. Ozon, J. P. Cusu, M. Anastasescu, V. A. Surdu, J. C. Moreno and A. M. Musuc, "High-Content *Aloe vera* Based Hydrogels: Physicochemical and Pharmaceutical Properties", *Polymers*, vol. 15, no. 5, (2023), p. 1312.
- [25] D. N. Iqbal, A. Munir, M. Abbas, A. Nazir, Z. Ali, S. Z. Alshawwa, M. Iqbal and N. Ahmad, "Polymeric Membranes of Chitosan *Aloe vera* Gel Fabrication with Enhanced Swelling and Anti-microbial Properties for Biomedical Applications", *Dose-Response*, vol. 21, no. 2, (2023), p. 15593258231169387.
- [26] I. Erol, Ö. Hazman, M. Aksu and I. Uygur, "Novel Bionanocomposites for Chitosan-Based Blend Containing L_aB_6 : Thermal, Dielectric, and Biological Properties", *Polymer for Advanced Technologies*, vol. 34, no. 8, (2023), pp. 2721-2738.
- [27] Y. Lin, C. Dong, F. Cao, L. Xiong, H. Gu and H. Xu, "Size-Dependent Optical Properties of Conjugated polymer nanoparticles", *RSC Advances*, vol. 7, no. 88, (2017), pp. 55957-55965.